Journal of Materials Chemistry A

Accepted Manuscript

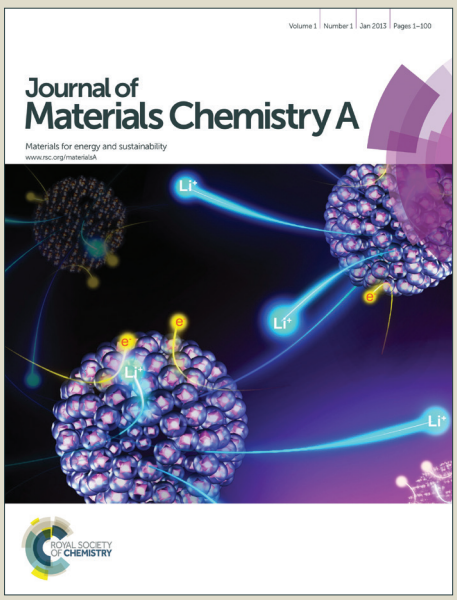

ROYAL SOCIETY OF CHEMISTRY

www.rsc.org/materialsA

Cite this: DOI: 10.1039/c0xx00000x

www.rsc.org/xxxxxx

Communication

Facile Synthesis of AgAuPd/Graphene with High Performance for Hydrogen Generation from Formic Acid

Si-jia Li, Yun Ping, Jun-Min Yan,* Hong-Li Wang, Ming Wu and Qing Jiang

Received (in XXX, XXX) Xth XXXXXXXXX 20XX, Accepted Xth XXXXXXXXX 20XX

DOI: 10.1039/b000000x

AgAuPd nanoparticles with small particle size, good dispersity and high degree of crystallinity on graphene are synthesized by a facile co-reduction route. The resultant AgAuPd/graphene exhibit 100% H_2 selectivity, 100% conversion and excellent catalytic activity toward the hydrogen generation form decomposition of formic acid without any additive at room temperature.

Hydrogen (H_2) is capable of providing highly stable, efficient and pollution-free power.[1] Its potential applications in onboard automotive industry and stationary power generation are promising.[2] However, H_2 generation from renewable sources and its secure storage remain as a big challenge in the H_2 energy based economy.[3] Formic acid (FA, HCOOH), as a promising H_2 storage material with nontoxicity, high energy density, excellent stability, and possible regenerability by hydrogenation of carbon dioxide (CO_2), has attracted much research interest.[4,5] H_2 can be generated by catalytic dehydrogenation of FA with the byproduct of CO_2.[4] The undesirable dehydration of FA to generate carbon monoxide (CO) should be avoided.[4,6]

Recently, many homogeneous and heterogeneous catalysts have been intensely investigated to increase the kinetic property of the dehydrogenation of FA at the mild reaction condition.[4,7] For example, metal complex-based homogeneous catalysts have been reported to have high performance for the formic acid decomposition at near-ambient temperatures.[4,8] Generally, heterogeneous nanocatalysts have the superiorities on controlling, retrieving, and recycling issues during or after reactions.[6,9] Therefore, there is a strong desire to develop heterogeneous catalysts with high activity and selectivity for the formic acid decomposition under mild conditions.[9,10] The performance of nanocatalyst is highly depended on its particle size, dispersion, crystallinity, support and etc.[11, 12] Herein we report a facile, eco-friendly, one-pot method for the synthesis of the reduced graphene oxide (rGO) supported AgAuPd ultrafine nanoalloy (~3 nm) with good dispersion and crystallinity (AgAuPd/rGO) by simultaneous reduction using ethanol as the reduction agent. The prepared AgAuPd/rGO exhibits the 100% H_2 selectivity, and high activity toward H_2 generation from FA without any additive at 298 K.

Graphene oxide (GO) aqueous solution is firstly prepared using the modified Hummers' method as the graphene precursor.[13] AgAuPd/rGO is synthesized by coreduction of GO and the metal precursors of Ag, Au and Pd, as illustrated in Scheme 1. Typically, for preparation of $Ag_{0.2}Au_{0.4}Pd_{0.4}$/rGO, 5.0 mL of aqueous solution containing $AgNO_3$ (0.02 mmol), Na_2PdCl_4 (0.04 mmol) and $HAuCl_4$ (0.04 mmol) was added into the well dispersed GO aqueous solution (32.5 mg, 45 mL), and then 40 mL of ethanol was added into above solution. The PH of the solution was adjusted to be 9-10 by adding KOH (1.0 M) aqueous solution. The solution was refluxed in an water bath at 353 K for 3 h with stirring. After 3 h, the obtained product is washed with water for several times and re-dispersed in 10 mL of water for the catalytic H_2 generation from the FA aqueous solution at 298 K. Additionally, AgAuPd/rGO with different Ag:Au:Pd molar ratio, the physical mixture of $Ag_{0.2}Au_{0.4}Pd_{0.4}$ and rGO, Pd/rGO and rGO were also synthesized through the same method mentioned above for comparation. Since pure graphene tends to aggregate due to its π - π stacking interactions,[17a] various effors have been made to avoid the aggration of graphene based catalysts, including electrostatic stabilization, chemical functionalization and adhering metal nanoparticles (NPs) on graphene sheets.[17a-c] The present co-reduction method to prepare AgAuPd/rGO may has the priority to suppress the aggration of rGO because the *in situ* generated NPs can increase the interlayer spacing between rGO sheets.[17d]

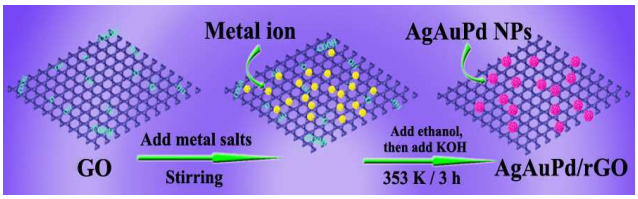

Scheme 1 Schematic illustration for preparation of AgAuPd/rGO

The morphology of the as-prepared specimens, $Ag_{0.2}Au_{0.4}Pd_{0.4}$/rGO composite and $Ag_{0.2}Au_{0.4}Pd_{0.4}$ NPs are characterized by transmission electron microscopy (TEM). It can be seen that the $Ag_{0.2}Au_{0.4}Pd_{0.4}$ NPs supported on rGO are well dispersed with an average particle size of about 3.0nm (Fig. 1a and b), while the NPs without rGO are seriously aggregated (Fig. 1d), suggesting that rGO lead to the good dispersion of $Ag_{0.2}Au_{0.4}Pd_{0.4}$ NPs on its surface. The high-resolution TEM (HRTEM) image reveals the crystalline

nature of the $Ag_{0.2}Au_{0.4}Pd_{0.4}$ NPs on rGO, and the lattice spacing is measured to be 0.231 nm （Fig. 1c）, which is between those of the (111) planes of face-centered cubic (fcc) Au (0.235 nm, JCPDS file:65-8601), Ag (0.235 nm, JCPDS file:65-2871) and Pd (0.224 nm, JCPDS file:65-2867).[14] And this reveals the formation of AgAuPd trimetallic alloy structure. Moreover, the X-ray diffraction (XRD) pattern of $Ag_{0.2}Au_{0.4}Pd_{0.4}$/rGO composite (Fig. 1e) shows that, besides the peak of (002) plane of rGO,[14c] all diffraction peaks can be assigned to (111), (200), (220) and (311) planes of a fcc strcture located between fcc Ag, Au and Pd, which further proves that the $Ag_{0.2}Au_{0.4}Pd_{0.4}$ is formed as an alloy. The accurate molar ratio of Ag:Au:Pd is determined to be 0.17:0.34:0.49 by inductively coupled plasma-atomic emission spectrometry (ICP-AES), which is close to the appointed value. Based on the above analyses, $Ag_{0.2}Au_{0.4}Pd_{0.4}$ nanoalloy supported on rGO has been succesfully synthesized by the present facile method.

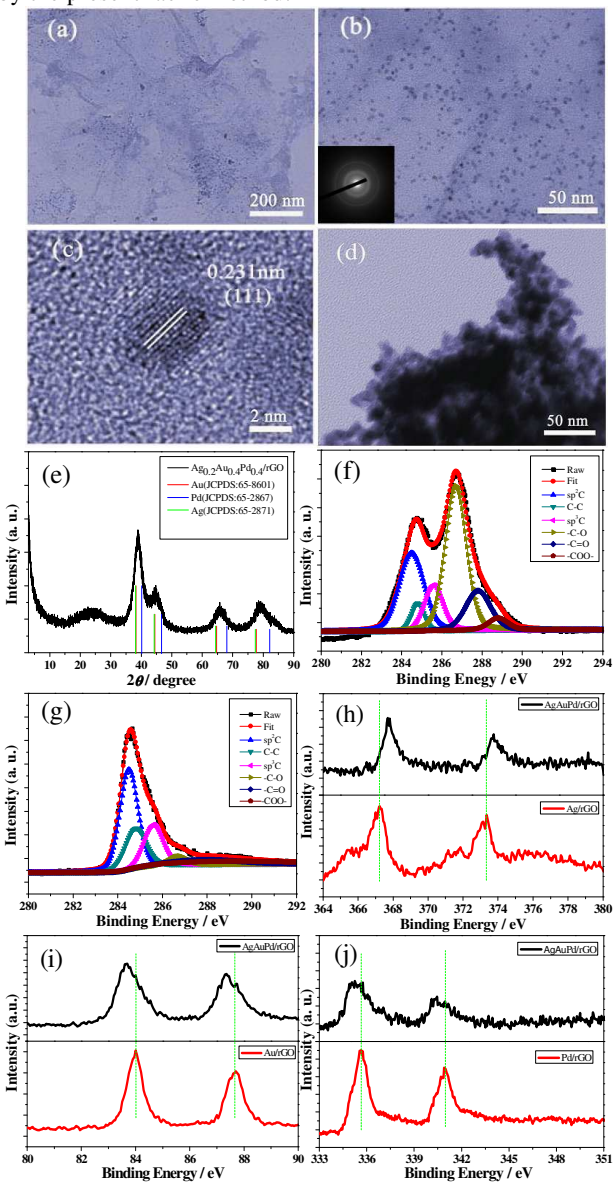

Fig. 1 TEM images with the (a) low, (b) middle, (c) high resolutions for $Ag_{0.2}Au_{0.4}Pd_{0.4}$/rGO (Fig. 2b inset: the corresponding SAED pattern for $Ag_{0.2}Au_{0.4}Pd_{0.4}$/rGO); (d) TEM images for free $Ag_{0.2}Au_{0.4}Pd_{0.4}$ NPs; (e) XRD pattern of $Ag_{0.2}Au_{0.4}Pd_{0.4}$/rGO NPs; XPS spectra of C 1s in (f) GO and (g) $Ag_{0.2}Au_{0.4}Pd_{0.4}$/rGO; and XPS spectra of (h) Ag 3d for Ag/rGO and $Ag_{0.2}Au_{0.4}Pd_{0.4}$/rGO, (i) Au 4f for Au/rGO and $Ag_{0.2}Au_{0.4}Pd_{0.4}$/rGO, (j) Pd 3d for Pd/rGO and $Ag_{0.2}Au_{0.4}Pd_{0.4}$/rGO.

X-ray photoelectron spectroscopy (XPS) measurements are used to determine the compositions and chemical states of the $Ag_{0.2}Au_{0.4}Pd_{0.4}$/ rGO hybride. The result for C 1s of the as-prepared GO (Fig. 1f) indicates that six different peaks centered at 284.5, 284.8, 285.6, 286.7, 287.8 and 288.8 eV are observed, corresponding to sp^2C, C-C, sp^3C, -C-O, -C=O and –COO groups, respectively.[15,16] After reduction, the intensities of all the C 1s peaks binding to oxygen obviously decrease (Fig. 1g), revealing that most of the oxygen containing species are removed and the majority of the conjugated C networks are restored. This confirms the reduction of GO to rGO during the preparation of $Ag_{0.2}Au_{0.4}Pd_{0.4}$/rGO hybrid, which is consistent with the Raman (Fig. S1) and ultraviolet visible (UV-Vis, Fig. S2) specra. Additionally, the XPS results show that the binding energy for Ag 3d in $Ag_{0.2}Au_{0.4}Pd_{0.4}$/rGO is located at the higher value relative to that in Ag/rGO (Fig. 1h); while binding energies for Au 4f and Pd 3d in $Ag_{0.2}Au_{0.4}Pd_{0.4}$/rGO are shifted to the lower values compared with those in Au/rGO and Pd/rGO, respectively. These shifts demonstrate that some electrons are transferred from Ag to Au and Pd atoms in the $Ag_{0.2}Au_{0.4}Pd_{0.4}$/rGO alloy structure. Such electron transfer in $Ag_{0.2}Au_{0.4}Pd_{0.4}$/rGO has the potential to endow itself with the high activity to H_2 generation from FA at 298 K.

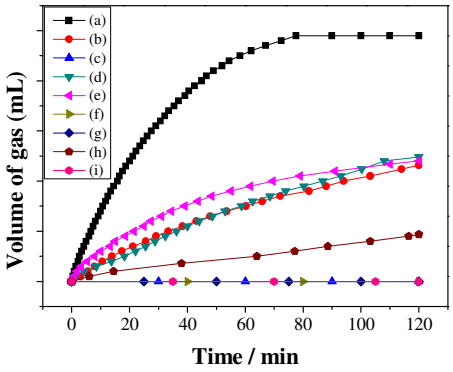

Fig. 2 Gas generation by the decomposition of FA (1 M, 5 mL) vs. time in the presence of (a) $Ag_{0.2}Au_{0.4}Pd_{0.4}$/rGO hybrid, (b) the physical mixture of $Ag_{0.2}Au_{0.4}Pd_{0.4}$ and rGO, (c) $Ag_{0.33}Au_{0.67}$/rGO, (d) $Ag_{0.33}Pd_{0.67}$/rGO, (e) $Au_{0.5}Pd_{0.5}$/rGO, (f) Ag/rGO, (g) Au/rGO, (h) Pd/rGO, (i) rGO at 298K under ambient atmosphere. (n_{metal}/n_{FA} = 0.02)

Fig. 2 shows the catalytic activities of $Ag_{0.2}Au_{0.4}Pd_{0.4}$/rGO hybrid, the physical mixture of $Ag_{0.2}Au_{0.4}Pd_{0.4}$ and rGO, bi-metallic ($Ag_{0.33}Au_{0.67}$/rGO, $Ag_{0.33}Pd_{0.67}$/rGO and $Au_{0.5}Pd_{0.5}$/rGO), mono-metallic (Ag/rGO, Au/rGO and Pd/rGO) counterparts and rGO for H_2 generation from FA decomposition at 298 K under ambient atmosphere. Obviously, the as-prepared $Ag_{0.2}Au_{0.4}Pd_{0.4}$/rGO hybrid exhibits the highest activity, with which 245 mL of gas can be released within 77.5 min without any additive at 298 K, corresponding to a conversion of 100%. Furthermore, the initial TOF over the $Ag_{0.2}Au_{0.4}Pd_{0.4}$/rGO composite is

measured to be 73.6 mol H_2 mol catalyst^{-1} h^{-1} at 298 K during the first 20 min, which is faster than most of the additive free heterogeneous catalysts ever reported at the room temperature. (Table S1)[6, 10h, 21, 23b, 23c, 24, 25] In contrast, the physical mixture ($Ag_{0.2}Au_{0.4}Pd_{0.4}$ and rGO) shows much lower activity, with which 110 mL of gas is obtained within 120 min. Over bimetallic $Ag_{0.33}Pd_{0.67}$/rGO and $Au_{0.5}Pd_{0.5}$/rGO catalysts, 124 and 120 mL gas can be released within 120 min, respectively, while $Ag_{0.33}Au_{0.67}$/rGO has no activity. With monometallic Pd/rGO, only 47 mL of gas can be generated within 120 min, whereas Au/rGO and Ag/rGO shows no activity. In addition, no gas is generated from FA in the case of only rGO, suggesting that rGO serve as a support for the growth of $Ag_{0.2}Au_{0.4}Pd_{0.4}$/rGO NPs, rather than catalysts for this reaction. Therefore, the enhanced catalytic performance of $Ag_{0.2}Au_{0.4}Pd_{0.4}$/rGO may be attributed to its special composition and surface electronic state in the alloy tructure as well as the small particle size and well dispersion due to the support of rGO. The generated gas over $Ag_{0.2}Au_{0.4}Pd_{0.4}$/rGO is identified by mass spectrometry (MS, Fig. S3) and gas chromatography (GC, Fig. S4) to be H_2 and CO_2 with the H_2: CO_2 molar ration of 1.0: 1.0, and no CO has been detected (Fig. S5, detection limit for CO: 10 ppm). This indicates the as-synthesized $Ag_{0.2}Au_{0.4}Pd_{0.4}$/rGO catalyst can catalyze FA aqueous solution decomposition into CO-free H_2, which is very important for fuel cell applications. To further determine the effect of the metal composition in system of AgAuPd/rGO on the catalytic performance, the molar ration of Ag: Au: Pd has been varied by several values. Setting the molar content of Ag as a constant of 0.2, $Ag_{0.2}Au_{0.8-x}Pd_x$/rGO system (x=0, 0.2, 0.4, 0.6, 0.8) reaches its highest activity when the molar ratio of Au:Pd is 1:1, namely, x is 0.4 (Figure S6). And then, setting the molar ratio of Au:Pd as 1:1, $Ag_{1-2y}Au_yPd_y$/rGO (y= 0.5, 0.4, 0.3, 0.25, 0.2, and 0) shows the best performace when the Ag molar content is 0.2, namely, y is 0.4 (Figure S7). As a result, once the ratio of Ag: Au: Pd is changed from 0.2: 0.4: 0.4, the resultant AgAuPd/rGO shows the decreased catalytic performance, and can not lead to the full conversion of FA within 120 min.

In order to demonstrate the advantages of ethanol as the reducing agent, we use similar method to synthesize $Ag_{0.2}Au_{0.4}Pd_{0.4}$/rGO NPs with $NaBH_4$ as the reducing agent, and the reducing temperature is 353 K and 298 K respectively. As shown in Fig. S8, the NPs reducing at 353 K have a larger average size of about 6.19 nm with severe aggregation, and the dispersion is very poor. The NPs reducing at 298 K have a mean size of about 3.40 nm with good dispersion, which is similar to the $Ag_{0.2}Au_{0.4}Pd_{0.4}$ NPs with ethanol reducing at 353 K. The corresponding SAED patterns (Fig. 2b inset, Fig. S8b inset, Fig. S8d inset) of the three specimens reveal that all of them are crystallized. However, as seen from their XRD patterns (Fig. S9), $Ag_{0.2}Au_{0.4}Pd_{0.4}$ reduced by ethanol at 353 K shows the best crystallinity, and that reduced by $NaBH_4$ at 298 K has the lowest crystallinity. The accurate molar ratios of Ag:Au:Pd in $Ag_{0.2}Au_{0.4}Pd_{0.4}$/rGO reduced by $NaBH_4$ at 353 K and 298 K (determined by ICP-AES) are 0.20:0.32:0.48 and 0.20:0.33:0.47, respectively, which are near to that in $Ag_{0.2}Au_{0.4}Pd_{0.4}$/rGO reduced by ethanol at 353 K. Moreover, the XPS spectra of Ag, Au, and Pd in the three specimens show the similar eletronic states with no obvious peak shift (Fig. S11). The catalytic activities of the there specimens for hydrogen generation from FA at 298 K are presented in Fig. S10 for comparasion. It can be seen that, within 90 min, only 150 mL of gas can be generated over $Ag_{0.2}Au_{0.4}Pd_{0.4}$/rGO reduced by $NaBH_4$ at 353 K, and no gas was obtained with catalyst reduced by $NaBH_4$ at 298 K. Therefore, it can be conclued that the small particle size, good dispersity and high degree of crystallinity due to the present synthetic method result in the excellent catalytic performace of $Ag_{0.2}Au_{0.4}Pd_{0.4}$/rGO.

In summary, $Ag_{0.2}Au_{0.4}Pd_{0.4}$ NPs decorated on rGO with small particle size, good dispersity and high degree of crystallinity are successfully synthesized by co-reduction of GO and the metal precursors using ethanol as the reduction agent at 353 K. The resultant $Ag_{0.2}Au_{0.4}Pd_{0.4}$/rGO composite shows 100% conversion, 100% H_2 selectivity, and excellent activity for dehydrogeneration of FA in aqueous solution without any additive at room temperature. This improvement in the catalytic performance of the $Ag_{0.2}Au_{0.4}Pd_{0.4}$/rGO composite may strongly encourage the practical application of FA as a promising H_2 storage material.

Acknoeledgements

This work was supported in part by theNational Natural Science Foundation of China (51471075, 51401084 and 51101070); National Key Basic Research, Development Program(2010CB631001).

Notes and references

Key Laboratory of Automobile Materials Ministry of Education, Department of Materials Science and Engineering Jilin University, Changchun 130022, China; E-mail: junminyan@jlu.edu.cn

† Electronic Supplementary Information (ESI) available: experimental procedures; Raman, UV-Vis, XPS, TEM, MS and GC, XRD data; TOF and conversion data; and the results of H_2 generation from FA. See DOI: 10.1039/b000000x/

[1] (a) L. Schlapbach and A. Zűttel, *Nature,* 2001, **414**, 353-358; (b) J. A. Turner, *Science,* 2004, **305**, 972-974.

[2] T. M. McCormick, B. D. Calitree, A. Orchard, N. D. Kraut, F. V. Bright, M. R. Detty and R. Eisenberg, *J. Am. Chem. Soc.,* 2010, **132**, 15480–15483.

[3] (a) P. Z. Li, A. Aijaz and Q. Xu, *Angew. Chem., Int. Ed.,* 2012, **51**, 6753-6756; (b) M. Yurderi, A. Bulut, M. Zahmakiran and M. Kaya, *Appl. Catal. B- Enciron*., 2014, **160-161**, 514-524.

[4] (a) B. Loges, A. Boddien, H. Junge and M. Beller, *Angew. Chem., Int. Ed.,* 2008, **47**, 3962-3965; (b) B. Loges, A. Boddien, F. Gärtner, H. Junge and M. Beller, *Top. Catal.,* 2010, **53**, 902-914; (c) M. Yadav and Q. Xu, *Energy Environ. Sci.,* 2012, **5**, 9698-9725; (d) C. Hu, S. W. Ting, J. Tsui and K. Y. Chan, *Int. J. Hydrogen Energy,* 2012, **37**, 6372-6380.

[5] (a) T. C. Johnson, D. J. Morris and M. Wills, *Chem. Soc. Rev.,* 2010, **39**, 81-88; (b) S. Enthaler, J. Von Langermann and T. Schmidt, *Energy Environ. Sci*., 2010, **3**, 1207-1217; (c) A. Boddien, D. Mellmann, F. Gärtner, R. Jackstell, H. Junge, P. J. Dyson, G. Laurenczy, R. Ludwig and M. Beller, *Science,* 2011, **333**, 1733-1736.

[6] K. Tedsree, T. Li, S. Jones, C. W. A. Chan, K. M. K. Yu, P. A. J. Bagot, E. A. Marquis, G. D. W. Smith and S. C. E. Tsang, *Nat.*

Nano., 2011, **6**, 302-307.

[7] J. F. Hull, Y. Himeda, W. H. Wang, B. Hashiguchi, R. Periana, D. J. Szalda, J. T. Muckerman and E. Fujita, *Nat. Chem.,* 2012, **4**, 383-388.

[8] (a) S. Fukuzumi, T. Kobayashi and T. Suenobu, *J. Am. Chem. Soc*., 2010, **132**, 1496-1497; (b) Y. Huang, X. Zhou, M. Yin, C. Liu and W. Xing, *Chem. Mater.,* 2010, **22**, 5122 – 5128.

[9] (a) A. Boddien and H. Junge, *Nat. Nanotechnol*., 2011, **6**, 265-266; (b) Z. L. Wang, J. M. Yan, H. L. Wang, Y. Ping and Q. Jiang, *J. Mater. Chem. A,* 2013, **1**, 12721-12725; (c) K. Mori, M. Dojo and H. Yamashita, *ACS Catal.,* 2013, **3**, 1114-1119; (d) Q. L. Zhu, N. Tsumori and Q. Xu, *Chem. Sci*., 2014, **5**, 195-199.

[10] (a) X. Zhou, Y. Huang, W. Xing, C. Liu, J. Liao and T. Lu, *Chem. Commun.,* 2008, 3540-3542; (b) M. Ojeda and E. Iglesia, *Angew. Chem*., Int. Ed., 2009, **121**, 4894-4897; (c) X. Gu, Z.H. Lu, H. L. Jiang, T. Akita and Q. Xu, *J. Am. Chem. Soc.,* 2011, **133**, 11822-11825; (d) M. Yadav, T. Akita, N. Tsumori and Q. Xu, *J. Mater. Chem.,* 2012, **22**, 12582-12586; (e) Q. Y. Bi, X. L. Du, Y. M. Liu, Y. Cao, H. Y. He and K. N. Fan, *J. Am. Chem. Soc.,* 2012, **134**, 8926-8933; (f) Z. L. Wang, J. M. Yan, H. L. Wang, Y. Ping and Q. Jiang, *Sci. Rep*., 2012, **2**, 598-603; (g) Ö. Metin, X. Sun and S. Sun, *Nanoscale,* 2013, **5**, 910-912; (h) Z. L. Wang, J. M. Yan, Y. Ping, H. L. Wang, W. T. Zheng and Q. Jiang, *Angew. Chem., Int. Ed.,* 2013, **52**, 4406-4409; (i) S. Zhang, Ö. Metin, D. Su and S. Sun, *Angew. Chem., Int. Ed.,* 2013, **52**, 3681-3684.

[11] (a) Y. H. Zheng, C. Q. Chen, Y. Y. Zhan, X. Y. Lin, Q. Zheng, K. M. Wei and J. F. Zhu, *J. Phys. Chem. C,* 2008, **112**, 10773-10777; (b) Y. J. Li, Y. J. Li, E. B. Zhu, T. McLouth, C. Y. Chiu, X. Q. Huang and Y. Huang, *J. Am. Chem. Soc*., 2012, **134**, 12326-12329; (c) P. Song, L. Liu, A. J. Wang, X. Zhang, S. Y. Zhou and J. J. Feng, *Electrochim. Acta*, 2015, **164**, 323-329; (d) H. Wu, S. Mei, X. Cao, J. Zheng, M. Lin, J. Tang, F. Ren, Y. Du, Y. Pan and H. Gu, *Nanotechnology*, 2014, **25**, 195702; (e) B. Sheng, L. Hu, T. Yu, X. Cao and H. Gu, *RSC Adv*., 2012, **2**, 5520-5523.

[12] (a) Y. Chen, Q. L. Zhu, N. Tsumori and Q. Xu, *J. Am. Chem. Soc*., 2015, **137**, 106-109; (b) F. Wang, C. H. Li, L. D. Sun, H. S. Wu, T. Ming, J. F. Wang, J. C. Yu and C. H. Yan, *J. Am. Chem. Soc.,* 2011, **133**, 1106-1111; (c) Y. L. Qin, J. Wang, F. Z. Meng, L. M. Wang and X. B. Zhang, *Chem. Commun*., 2013, **49**, 10028-10030; (d) B. Y. Xia, Y. Yan, X. Wang and X. W. Lou, *Mater. Horiz*., 2014, **1**, 379.

[13] D. C. Marcano, D. V. Kosynkin, J. M. Berlin, A. Sinitskii, Z. Sun, A. Slesarev, L. B. Alemany, W. Lu and J. M. Tour, *ACS Nano,* 2010, **4**, 4806–4814.

[14] (a) Z. L. Wang, H. L. Wang, J. M. Yan, Y. Ping, S. I. O, S. J. Li, Q. Jiang, *Chem. Commun*., 2014, **50**, 2732-2734; (b) Y. Y. Wen, H. M. Ding, Y. K. Shan, *Nanoscale,* 2011, **3**, 4411-4417; (c) P. Bhunia, G. Kim, C. Baik and H. Lee, *Chem. Commun.,* 2012, **48**, 9888-9890.

[15] Y. H. Ng, A. Iwase, N. J. Bell, A. Kudo and R. Amal, *Catal. Today,* 2011, **164**, 353-357.

[16] Z. J. Fan, W. Kai, J. Yan, T. Wei, L. J. Zhi, J. Feng, Y. M. Ren, L. P. Song and F. Wei, *ACS Nano,* 2011, **5**, 191–198.

[17] (a) B. Y. Xia, B. Wang, H. B. Wu, Z. Liu, X. Wang and X. W. Lou, *J. Mater. Chem*., 2012, **22**, 16499-16505; (b) P. V. Kamat, *J. Phys. Chem. Lett*., 2010, **1**, 520-527; (c) Y. Si and E. T. Samulski, *Chem. Mater*., 2008, **20**, 6792-6997; (d) R. Pasricha, S. Gupta and A. K. Srivastava, *Small*, 2009, **5**, 2253-2259.

[18] M. Yadav, A. K. Singh, N. Tsumori and Q. Xu, *J. Mater. Chem,* 2012, **22**, 19146-19150.

[19] S. W. Ting, S. Cheng, K. Y. Tsang, N. van der Laak and K. Y. Chan, *Chem. Commun*., 2009, 7333-7335.

[20] J. H. Lee, J. Ryu, J. Y. Kim, S. W. Nam, J. Han, T. H. Lim, S. Gautam, K. H. Chae and C. W. Yoon, *J. Mater. Chem. A,* 2014, **2**, 9490-9495.

[21] Y. Y. Cai, X. H. Li, Y. N. Zhang, X. Wei, K. X. Wang and J. S. Chen, *Angew. Chem*., 2013, **125**, 12038-12041.

[22] Y. Ping, J. M. Yan, Z. L. Wang, H. L. Wang and Q. Jiang, *J. Mater. Chem. A,* 2013, **1**, 12188-12191.

[23] (a) J. M. Yan, Z. L. Wang, L. Gu, S. J. Li, H. L. Wang, W. T. Zheng and Q. Jiang, *Adv. Energy Mater*., 2015, DOI: 10.1002/aenm: 201500107; (b) Z. L. Wang, Y. Ping, J. M. Yan, H. L. Wang and Q. Jiang, *Int. J. Hydrogen Energy,* 2014, **39**, 4850-4856; (c) Z. L. Wang, J. M. Yan, Y. F. Zhang, Y. Ping, H. L. Wang and Q. Jiang *Nanoscale*, 2014, **6**, 3073-3077.

[24] C. Q. Hu, J. K. Pulleri, S. W. Ting and K. Y. Chan, *Int. J. Hydrogen Energy*, 2014, **39**, 381-390.

[25] S. Jones, J. Qu, K. Tedsree, X. Q. Gong and S. C. E. Tsang, *Angew. Chem, Int. Ed.,* 2012, **51**, 11275-11278.

Table of Contents Entry

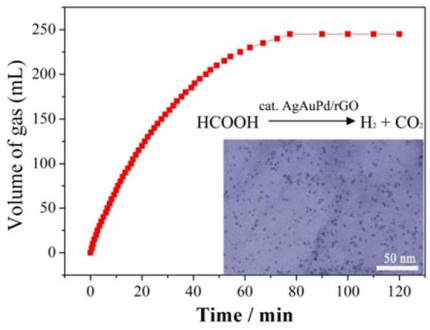

Well dispersed and ultrafine AgAuPd nanoalloy supported on rGO shows excellent catalytic performance toward hydrogen generation from formic acid decomposition.